Japanese Journal of Applied Physics **50** (2011) 030203 **RAPID COMMUNICATION**
DOI: 10.1143/JJAP.50.030203

Terahertz Birefringence in Zinc Oxide

Youngchan Kim[1,2], Jaewook Ahn[1]*, Bog G. Kim[3], and Dae-Su Yee[2]*,†

[1]*Department of Physics, Korea Advanced Institute of Science and Technology, Daejeon 305-701, Korea*
[2]*Center for Safety Measurements, Korea Research Institute of Standards and Science, Daejeon 305-340, Korea*
[3]*Department of Physics, Pusan National University, Busan 609-735, Korea*

Received January 13, 2011; accepted January 26, 2011; published online March 7, 2011

The birefringence of zinc oxide (ZnO) in the terahertz (THz) frequency range is measured using a parallel-polarization configuration THz time-domain spectrometer and compared with the result of an *ab initio* calculation. The measured birefringence of 0.180 at 1 THz shows good agreement with the calculated value of 0.170 from full phonon consideration, both of which are about 20 times larger than the birefringence in the visible range. It is found that the difference of the transverse optical and longitudinal optical (TO–LO) phonon splitting between the optical phonon branches (A_1 and E_1) predominantly contributes to the huge birefringence of ZnO in the THz frequency region.

Over the past two decades, terahertz time-domain spectroscopy (THz-TDS) has become one of the essential analyzing tools in material science.[1)] Many materials extending from gases and liquids to solid-state and biological media have complex dielectric response in the terahertz (THz) frequency range of 0.1 to 10 THz, and therefore, a whole range of useful applications become promising in this spectral range in particular for next-generation communications, medical imaging, and security purposes.[2,3)] There exist many reports on THz dielectric properties of materials, and more advanced optical properties such as birefringence, optical activity, and magneto/electro-optical effects in the THz range are less studied and under active investigation.[4)]

Recently, THz wave generation was demonstrated from a ZnO photoconductive antenna excited by ultraviolet pulses,[5)] and the far-infrared optical and dielectric properties of ZnO were experimentally characterized by use of THz-TDS.[6)] ZnO has a number of advantages for THz photonics: wide bandgap, high breakdown voltage, high resistivity and mobility, optical transparency, and easy fabrication. Although there exist a lot of reports on the optical properties of ZnO,[6–8)] there is no experimental report on THz birefringence of ZnO.

In this study, we report the extraordinary and ordinary refractive indices (n_e and n_o) as well as the absorption coefficients of a ZnO single crystal in the frequency region of 0.25–1.35 THz. For this, azimuthal angle dependence of transmission has been measured in a parallel-polarization configuration THz time-domain spectrometer and the experimental result is compared with an *ab initio* calculation of dielectric and optical properties.

ZnO has the hexagonal wurtzite structure with each Zn ion in a tetrahedron of O ions. This tetrahedral structure has polar symmetry along the hexagonal *c*-axis of ZnO,[9)] and thus, birefringence occurs for a THz wave propagating normal to the $(10\bar{1}0)$ crystal surface and not to the (0001) surface. We used a both-side polished 2-mm-thick ZnO single crystal with a $10 \times 10\,\mathrm{mm}^2$ area in the $\langle 10\bar{1}0 \rangle$ orientation. For a precision measurement of THz birefringence in ZnO, asynchronous-optical-sampling THz-TDS was used in transmission geometry.[10,11)] Two low-temperature-grown GaAs photoconductive antennas were used for emission and detection of pulsed THz waves. A pulsed THz wave linearly polarized along the vertical axis, which is emitted from the biased THz emitter, is focused on the ZnO sample with a spot size of ~2 mm. The THz wave transmitted through the ZnO sample is detected by the THz detector that is oriented so as to detect only the vertical component of the electric field. The enclosure containing the THz beam path is purged with dry air to eliminate the absorption by water vapor in ambient air.

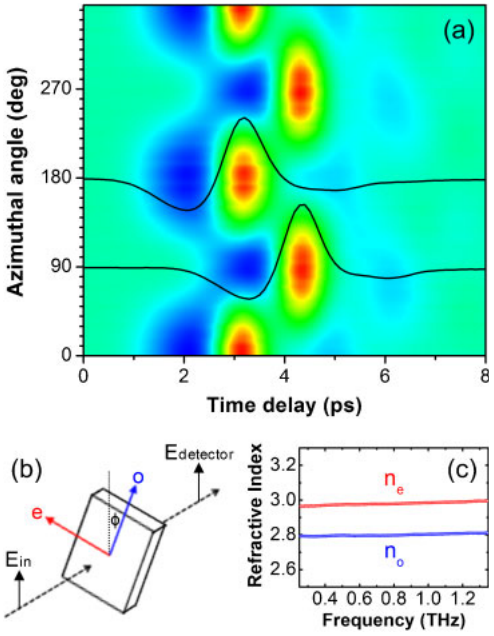

Fig. 1. (Color online) (a) Transmitted THz waveforms measured with varying the azimuthal angle ϕ of the ZnO sample in the parallel-polarization configuration illustrated in (b), and (c) measured extraordinary and ordinary refractive indices of the ZnO sample. The solid curves in (a) represent the waveforms measured at 90 and 180°, respectively.

The reference (input) and transmitted (output) THz pulses are measured without and with the ZnO sample, respectively. Figure 1(a) shows the transmitted THz waveforms measured with rotating the sample in the parallel-polarization configuration that is described above and illustrated in Fig. 1(b). The time delay position of the THz pulse oscillates with a 180° period of the azimuthal angle, which implies the existence of birefringence. Using Fourier analysis of input and output pulses, we can obtain the frequency-dependent

*The authors have the same responsibilities for this paper.
†E-mail address: dsyee@kriss.re.kr

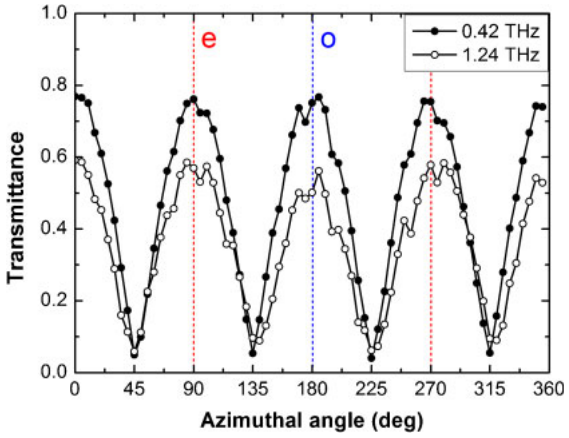

Fig. 2. (Color online) Azimuthal angle dependence of the amplitude transmittance of the ZnO sample at 0.42 and 1.24 THz, measured in the parallel-polarization configuration. The 0° (180°) and 90° (270°) orientations represent ordinary and extraordinary waves, respectively.

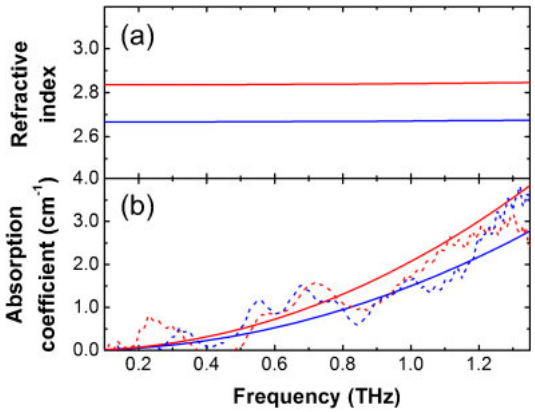

Fig. 3. (Color online) (a) Refractive indices and (b) absorption coefficients of ZnO in the THz region for the extraordinary (red curve) and ordinary (blue curve) waves, obtained from the *ab initio* calculation. The dashed curves in (b) indicate experimental results.

refractive index, $n(\omega)$, and absorption coefficient, $\alpha(\omega)$, given by

$$n(\omega) = 1 + \frac{c\theta(\omega)}{\omega L}, \tag{1}$$

$$\alpha(\omega) = \frac{2}{L}\ln\left\{\frac{4n(\omega)}{T(\omega)[n(\omega)+1]^2}\right\}, \tag{2}$$

where L is the crystal thickness, c is the speed of light in vacuum, and T and θ are defined as $Te^{-i\theta} = E_{\text{output}}(\omega)/E_{\text{input}}(\omega)$.[12] To remove the Fabry–Perot effect, the amplitude and phase spectra, of which the frequency resolution is 2.63 GHz, are smoothed using adjacent-averaging of 19 points, closely equal to twice the period of the Fabry–Perot ripple on the spectra. Figure 1(c) shows the dispersion of n_e and n_o of the ZnO sample. The birefringence defined by $\Delta n = n_e - n_o$ is measured 0.180 ± 0.003 in the frequency region of 0.25–1.35 THz.

The birefringence causes the phase retardation ($\Delta\theta$) between the ordinary and extraordinary waves given by $\Delta\theta = \omega L \Delta n/c$. Figure 2 displays the azimuthal angle dependence of the amplitude transmittance (from 0 to 360° at a step of 5°) at 0.42 and 1.24 THz, measured in the parallel-polarization configuration. The transmittances have maximum values at the 0°, 90°, and equivalent orientations without change in the polarization before and after transmission through the ZnO sample. In contrast, half-wave phase retardation makes the transmittances reach minima at the 45°, 135°, and equivalent orientations, rotating the polarization by 90°. Thus, the ZnO crystal of 2 mm thickness can be used as a half-wave plate at 0.42 and 1.24 THz, and also a quarter-wave plate at 0.62 and 1.03 THz. Certainly, further design is required for broadband applications.[13]

In order to understand the giant THz birefrigence in ZnO, we carried out an *ab initio* phonon calculation using CRYSTAL09[14] which employed a hybrid exchange-correlation function B3LYP[15] and a localized basis set of Gaussian type functions (GTFs). All electron GTFs were used for Zn[16] and O.[17] The bandgap was calculated ~3.23 eV with full optimization of the lattice constant and oxygen position, in good agreement with the recent calculation of Du and Zhang.[18]

The birefringence in the optical region (~1 eV range) is related to the crystal symmetry and ZnO belongs to the uniaxial system with $\varepsilon_{xx} = \varepsilon_{yy} \neq \varepsilon_{zz}$. We performed the coupled perturbed Kohn-Sham calculation[19] to get the dielectric constant tensor in the visible region; $\varepsilon_{xx} = \varepsilon_{yy} = 3.3891$ and $\varepsilon_{zz} = 3.4213$, which give $n_o = n_{xx} = \sqrt{\varepsilon_{xx}} = 1.8410$, $n_e = n_{zz} = \sqrt{\varepsilon_{zz}} = 1.8497$, and the birefringence of 0.0087. Since ZnO has ionicity,[20] the birefringence in the THz region is related to the difference of the transverse optical and longitudinal optical (TO–LO) phonon splitting between the zone center optical phonons (A_1 and E_1) in the infrared region (few hundred wavenumber) in addition to the birefringence in the optical region. In order to calculate the birefringence in the THz region, full phonon calculations were performed.[21] For ZnO having the wurtzite structure, it is well known that the non-degenerate A_1 and doubly degenerate E_1 modes are infrared active. Our calculation shows that the LO (TO) phonon frequency of the A_1 mode is 589.18 cm^{-1} (384.31 cm^{-1}) and the LO (TO) phonon frequency of the E_1 mode is 606.38 cm^{-1} (418.05 cm^{-1}). The relative intensity ratio of the A_1 and E_1 modes is 664 : 1270.

Symmetry analysis shows that $\varepsilon_{xx} = \varepsilon_{yy} = n_o^2$ is related to the E_1 modes and $\varepsilon_{zz} = n_e^2$ to the A_1 modes. The dielectric constant tensor, $\varepsilon(\omega)$, in the THz region can be expressed in terms of the high-frequency dielectric constant tensor, $\varepsilon(\infty)$, the LO and TO phonon frequencies ($\omega_{E1,\text{LO}}$, $\omega_{E1,\text{TO}}$, $\omega_{A1,\text{LO}}$, and $\omega_{A1,\text{TO}}$), and the damping constant, γ:

$$\varepsilon_{xx}(\omega) = \varepsilon_{xx}(\infty)\frac{\omega_{E1,\text{LO}}^2 - \omega^2 - i\gamma\omega}{\omega_{E1,\text{TO}}^2 - \omega^2 - i\gamma\omega}, \tag{3}$$

$$\varepsilon_{zz}(\omega) = \varepsilon_{zz}(\infty)\frac{\omega_{A1,\text{LO}}^2 - \omega^2 - i\gamma\omega}{\omega_{A1,\text{TO}}^2 - \omega^2 - i\gamma\omega}. \tag{4}$$

Having the necessary information from the *ab initio* calculation and assuming $\gamma = 27.3\,\text{cm}^{-1}$ from ref. 6, calculations of the complex dielectric constant tensor in the THz region were performed. Figure 3(a) shows the real parts of the complex refractive indices of ZnO with respect to the two different polarizations: the extraordinary and ordinary refractive indices. The extraordinary and ordinary refractive

indices at 1 THz are 2.841 and 2.671, respectively, and thus, the birefringence at 1 THz is 0.170, which is about 20 times larger than the birefringence in the visible region. Our *ab initio* calculation reproduces the experimental results quite well and shows that the huge birefringence in the THz region originates from the difference of the TO–LO phonon splitting between the optical phonon branches (A_1 and E_1). As shown in Fig. 3(b), the absorption coefficients of ZnO for the two different polarizations, which are obtained from the imaginary parts of the complex refractive indices, also agree with the measured results. They are lower than 4 cm^{-1} in the given THz frequency range in accordance with the result in ref. 6 and the low absorption property of ZnO is of benefit to THz device applications.

In conclusion, we have studied the THz birefringence of the ZnO crystal with crystal orientation of $\langle 10\bar{1}0 \rangle$ using a THz time-domain spectrometer in a parallel-polarization configuration. The birefringence of ZnO measured about 0.180 in the 0.25–1.35 THz frequency range shows good agreement with the calculated value of 0.170 from the full phonon consideration. This huge birefringence of ZnO in the THz frequency region is well understood in conjunction with the TO–LO phonon splitting.

Acknowledgments This work was supported in part by the Industrial Strategic Technology Program of the Ministry of Knowledge Economy (KI001889) and in part by the Ministry of Education, Science, and Technology through project KRISS-10011131. Bog G. Kim acknowledges the support from National Research Foundation (NRF, NRF-2009-0070830 and NRF-2010-0001-226).

1) C. Fattinger and D. Grischkowsky: Appl. Phys. Lett. **54** (1989) 490.
2) B. Ferguson and X.-C. Zhang: Nat. Mater. **1** (2002) 26.
3) M. Tonouchi: Nat. Photonics **1** (2007) 97.
4) Y.-S. Lee: *Principles of Terahertz Science and Technology* (Springer, Heidelberg, 2009).
5) S. Ono, H. Murakami, A. Quema, G. Diwa, N. Sarukura, R. Nagasaka, Y. Ichikawa, H. Ogino, E. Ohshima, A. Yoshikawa, and T. Fukuda: Appl. Phys. Lett. **87** (2005) 261112.
6) A. K. Azad, J. Han, and W. Zhang: Appl. Phys. Lett. **88** (2006) 021103.
7) W. L. Bond: J. Appl. Phys. **36** (1965) 1674.
8) Y. S. Park and J. R. Schneider: J. Appl. Phys. **39** (1968) 3049.
9) C. Jagadish and S. J. Pearton: *Zinc Oxide Bulk, Thin Films and Nanostructures: Processing, Properties and Applications* (Elsevier, Amsterdam, 2006).
10) T. Yasui, E. Saneyoshi, and T. Araki: Appl. Phys. Lett. **87** (2005) 061101.
11) Y. Kim, D.-S. Yee, M. Yi, and J. Ahn: J. Korean Phys. Soc. **56** (2010) 255.
12) S. P. Mickan and X.-C. Zhang: Int. J. High Speed Electron. Syst. **13** (2003) 601.
13) J.-B. Masson and G. Gallot: Opt. Lett. **31** (2006) 265.
14) R. Dovesi, V. R. Saunders, C. Roetti, R. Orlando, C. M. Zicovich-Wilson, F. Pascale, B. Civalleri, K. Doll, N. M. Harrison, I. J. Bush, Ph. D'Arco, and M. Llunell: CRYSTAL09 User's Manual (University of Torino, Torino, 2009).
15) A. D. Becke: J. Chem. Phys. **98** (1993) 5648.
16) J. E. Jaffe and A. C. Hess: Phys. Rev. B **48** (1993) 7903.
17) M. D. Towler, N. L. Allan, N. M. Harrison, V. R. Saunders, W. C. Mackrodt, and E. Apra: Phys. Rev. B **50** (1994) 5041.
18) M.-H. Du and S. B. Zhang: Phys. Rev. B **80** (2009) 115217.
19) M. Ferrero, M. Rerat, R. Orlando, and R. Dovesi: J. Comput. Chem. **29** (2008) 1450.
20) Mulliken charge analysis shows that the charge of Zn ion is $+1.155e$ and that of oxygen is $-1.155e$, whereas Born charge tensor analysis, related with phonon vibration, shows that the Zn ion has $+2.056e$ dynamic charge and the Oxygen ion has $-2.056e$ dynamic charge.
21) F. Pascale, C. M. Zicovich-Wilson, F. L. Gejo, B. Civalleri, R. Orlando, and R. Dovesi: J. Comput. Chem. **25** (2004) 888.